X-ray Investigation of Low-Cycle Fatigue in Martensitic Steels

X-ray Investigation of Low-Cycle Fatigue in Martensitic Steels*

Yûnoshin IMAI and Shin-ichiro KUMAGAI

The Research Institute for Iron, Steel and Other Metals

(Received August 18, 1971)

Synopsis

Specimens of 0.38%C steel and Fe–25%Ni alloy were put to test of their low-cycle fatigue, tensile and hardness properties, both in their tempered state. The maximum bending strain on their surfaces under which the fatigue was tested was controlled at between 1.0 and 1.6%. The X-ray diffraction and thin film electronmicroscopy methods and some other techniques were employed for the purpose. The results obtained may be summarized in two phenomena. One is similar to the contrast of annealed metals versus cold-worked metals, and the other is what is considered to characterize the tempered martensite.

Both materials in tempered condition present a remarkable variation in microstructure, and the difference in microstructure is almost leveled out only in the low carbon 25%Ni alloy by the fatigue and this phenomenon is similar to the contrast of annealed metals versus cold-worked metals. But in the 0.38%C steel the difference is not leveled out even after the fatigue to failure.

The results obtained are not yet adequate enough to explain the correlation between the microstructural variation and the damage fraction in a tempered martensite. The crack initiation and propagation in the 0.38%C steel and 25%Ni alloy are often related longitudinally to the edges of martensite leaves.

I. Introduction

In recent years many investigations on microstructural changes during low-cycle fatigue test in metals have been carried out by using X-ray diffraction[1]~[5] and thin film electronmicroscopy methods[6]~[10], and have been attempted to correlate the microstructural changes to the damage fraction.

In the case of X-ray studies in the so-called high-cycle fatigue, it has already been well confirmed that the damage fraction can be presumed by the changes in a

---

* The **1513th** report of the Research Institute for Iron, Steel and Other Metals. Published in Japanese in the J. Soc. Mater. Sci., Japan, **19** (1970), 1121.

(1) S. Taira, T. Goto and Y. Nakano, The 11th Jap. Cong. Mat. Research (1968), 25.
(2) S. Taira, T. Goto and Y. Nakano, J. Soc. Mat. Sci., Japan, **17** (1968), 1135.
(3) S. Taira, T. Goto and Y. Mihara, ibid., **18** (1969), 385.
(4) S. Taira, T. Goto and Y. Mihara, ibid., **18** (1969), 1093.
(5) S. Taira, T. Goto and Y. Nakano, ibid., **19** (1970), 441.
(6) C.E. Feltner and C. Laird, Acta Met., **15** (1967), 15.
(7) P. Lukáš, M. Klesnil and P. Ryš, Z. Metallkde., **56** (1965), 109.
(8) M. Klesnil and P. Lukáš, J. Iron, Steel Inst., **203** (1965), 1043.
(9) C.E. Feltner and C. Laird, Czech. J. Phys., **B14** (1964), 600.
(10) R.W. Hinton, Trans. ASM, **61**(1968), 176.

half-value breadth of X-ray diffraction line in mild steel[11]. But in the low-cycle fatigue, it was found that the variation mode in half-value breadth was not the same as that in the high-cycle fatigue[12], and therefore, at present the half-value breadth is considered to be insufficient to presume the damage fraction[1], and more detailed consideration on the effects caused in X-ray diffraction line from a number of physical attributes such as the microstrain, particle size, excess dislocation density and misorientation are required[1]~[5]. In the thin film electronmicroscopic studies, all of their results were not yet sufficient to explain the correlation between the microstructural changes and the damage fraction both in high-cycle fatigue [13]~[24] and in low-cycle one[6]~[10].

In general, microstructures such as density and distribution of dislocations in tempered martensite detected by X-ray diffraction methods are similar to that in cold-worked metals. However, other metallurgical structures such as prior austenite grain boundaries, precipitated carbides, retained austenite, characteristic substructure of martensite leaves, etc. are found only in the microstructure of tempered martensite.

In this investigation, we have mainly observed the microstructural changes during low-cycle fatigue by means of the X-ray and thin film electronmicroscopy techniques in two kinds of tempered martensitic steels, that is, 0.38%C steel and 25%Ni alloy which scarcely contain the retained austenite, and attempted to obtain a preliminary information on the low-cycle fatigue properties which are expected to characterize martensite. And on the basis of the experimental results, for instance, on the half-value breadth, microstrain and particle size estimated from X-ray diffraction line, we briefly considered the possibility of a quantitative discussion on the low-cycle fatigue damage. Further, the relationships between the initiation or propagation sites of fatigue microcracks and the metallurgical microstructures on the surface of smooth specimens are also briefly included.

---

(11) The 2nd Division of the Committee for X-ray Study on Deformation and Fracture of Solid Materials, J. Soc. Mat. Sci., Japan, **18** (1969), 679.
(12) S. Taira and M. Kitagawa, The 5th Simposium on X-ray Investigation on Strength of Materials, Kyoto, Japan, Aug. 1966.
(13) C.E. Feltner, Phil. Mag., **8** (1963), 2121.
(14) G.W.J. Wardron, Acta Met., **13** (1965), 897.
(15) A. Yoshida et al., J. Soc. Mat. Sci., Japan, **18** (1969), 1106.
(16) J.T. McGrath and W.J. Bratina, Phil. Mag., **12** (1965), 1293.
(17) R.P. Wei and A.J. Baker, Phil. Mag., **12** (1965), 1005.
(18) J.T. McGrath and W.J. Bratina, Phil. Mag., **11** (1965), 429.
(19) O. Vingsbo et al., Phil. Mag., **17** (1968), 441.
(20) P. Lukaš and M. Klesnil, Czech. J. Phys., **B14** (1964), 600.
(21) J.E. Pratt, Acta Met., **15** (1967), 319.
(22) R.L. Segal, P.G. Partridge and P.B. Hirsch, Phil. Mag., **6** (1961), 1493.
(23) K. Mlesnil and P. Lukáš, Fracture, (1969), 725. Proc. 2nd Inter. Conf. on Fracture, Brighton.
(24) P.G. Forrest and L.M.T. Hopkin, N.P.L. Symposium No. **15** (1964), 348.

II. Experimental procedure

1. Material and specimens

The compositions of the medium carbon steel S38C and the vacuum melted 25Ni alloy used in this investigation are listed in Table 1.

Table 1. Chemical composition (wt%).

	C	Si	Mn	P	S	Cu	Cr	Ni
25Ni	0.003	0.001	tr.	0.001	0.002	–	–	25.18
S38C	0.38	0.25	0.71	0.01	0.010	0.08	0.06	–

Both materials in the form of a 3 mm×15 mm hot-rolled bar were cold-rolled to 0.22 mm in thickness. From these cold-rolled thin plate were prepared the specimens for tensile and low-cycle fatigue tests. A gauge section 10 mm×0.22 mm and 20 mm long was used for the tensile specimen, and the fatigue specimen was a rectangular thin plate in the size of 12 mm×35 mm×0.22 mm.

The S38C specimens were austenitized at 850°C in argon gas and then were quenched in ice water. These quenched specimens were tempered for 2 hours at various temperatures from 150° to 650°C. The 25Ni specimens were austenitized at 1000°C in vacuo and then water-quenched. After water-quenching, these specimens were immediately subzero-cooled to −196°C and then tempered for 1 hour at various temperatures from room temperature to 450°C at intervals of 150°C.

Table 2. Mechanical properties.

	Tempering	$\sigma_{0.2}$ (kg/mm²)	σ_B (kg/mm²)	δ (%)
25Ni	As Q.	55.0	79.1	6.2
	150°C	57.8	77.7	6.0
	300°C	68.4	76.8	7.8
	450°C	69.3	72.5	14.2
S38C	As Q.	–	–	–
	200°C	143	168	3.0
	275°C	135	154	3.5
	350°C	120	136	6.0
	450°C	98.5	103	8.4
	550°C	78.2	85.0	14.5
	650°C	60 4	67.5	21.0

* 25Ni: 1000°C WQ+Subzero Q+Tempering (×1hr)
S38C: 850°C WQ+Tempering (×2hrs)

After the heat treatment, the tensile and fatigue specimens were electropolished from each side of the plate to 0.20 mm in thickness. The tensile properties of tempered specimens used in this investigation were shown in Table 2. In the 25Ni specimens, yield strength ($\sigma_{0.2}$) increases with the rise of tempering temperature up to 450°C. Although we cannot definitely conclude this cause, but it may be

thought that the increase of yield strength is caused from some microstructural variations accompanied by a recovery effect and from precipitation of fine austenite phase, which has been clearly detected by X-ray diffraction methods, in the case of tempering at least at 450°C.

2. Experiments

Low-cycle fatigue tests were conducted by the method as shown in Fig. 1, that is, a fatigue specimen was placed crosswise between two cylinders of radius (r) and was alternately bent to coming in contact with the surface of cylinders

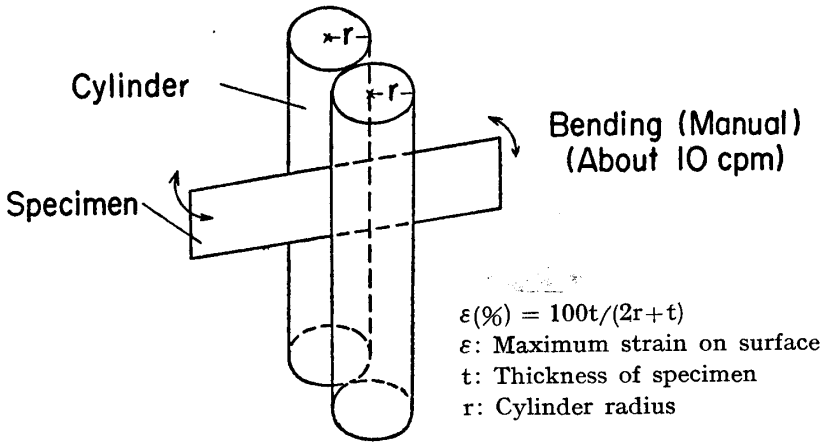

Fig. 1. Low-cycle fatigue testing method.

at 20°C. Tests were carried out at a frequency of about 10 cpm under the constant maximum bending strain (ε) of $\pm 1.0 \sim \pm 1.6\%$ on the surfaces of specimen. The value of ε was controlled according to radius (r) of cylinders and was calculated by the following equation, as shown in Fig. 1.

$$\varepsilon = 100t/(2r+t) \tag{1}$$

where (t) denotes the thickness of specimens (0.20 mm).

Fatigue tests were ceased, for a while, every at the appointed cycles in a state of contact with the surfaces of cylinder and specimen each other, and such a permanently deformed specimen was removed from the cylinders.

The permanent deflection of specimen induced by bending was measured and then was corrected in a flat state. In this flattened specimen, existence of fatigue microcracks was microscopically observed and the half-value breadth of X-ray diffraction line from $(211)\alpha'$ plane on the surface layer of specimen was measured. Besides this, particle size (D) and microstrain ($\Delta d/d$) measurements by X-ray method, substructure observations by thin film electronmicroscopy technique and micro-Vickers hardness test were carried out before every fatigue test and after cycling to failure on the surface layer of specimen.

For the measurement of half-value breadth, a film method by using back

Table 3. X-ray conditions.

		Half-value breadth	Particle size or Microstrain	
	Diffraction plane	(211)	(110)	(220)
	Characteristic X-ray	Cr-K_α	Cr-K_α	Co-K_α
	Filter	V	V	Fe
	Tube voltage (KV)	30	30	30
	Tube current (mA)	8	8	8
Diffracto-meter	Glancing angle (°)	—	6	6
	Scanning speed (2θ°/min)	—	0.2	0.2
	Slit divergence (°)	—	3	3
	Chart speed (mm/min)	—	10	10
	Time constant (sec)	—	0.5	0.5
Film	Collimator dia. (mm)	1.0	—	—
	Exposure time (min)	20	—	—
	Film	Fuji 200	—	—

diffraction camera was employed. And for the measurement of particle size and microstrain, a diffractometer method was employed. The diffraction line from (211)α', (110)α' and (220)α' planes were obtained under the conditions given in Table 3.

In the low temperature tempered specimens, broadening of diffraction lines is very large. In spite of difficulties in separation of the $K_{\alpha 1}$ diffraction line from such a broadened K_α doublet, the half-value breadth itself in the separated ones has no definite physical meaning. Therefore, in this report, the half-value breadth of (211)α' line was measured for convenience as the K_α doublet.

The particle size and microstrain broadening functions in the tempered martensite were assumed as Gaussian curves[25], and then, the particle size and microstrain were determined by the following equations.

$$\beta = \sqrt{B^2 - b^2} \tag{2}$$

$$(\beta \cos\theta/\lambda)^2 = (1/D)^2 + 16\,(\Delta d/d)^2\,(\sin\theta/\lambda)^2 \tag{3}$$

where β: Corrected integral breadth in the $K_{\alpha 1}$ line*

B: Measured integral breadth in the $K_{\alpha 1}$ line*

b: Integral breadth in the $K_{\alpha 1}$ line of the standard*

λ: Wavelength of X-ray

θ: Bragg angle

* In order to separate the $K_{\alpha 1}$ diffraction line from K_α doublet, Rachinger's method[26] were employed.

The influence of stacking fault on the value of particle size[27] was not considered

(25) F.E. Wetner, B.L. Averbach and Morris Cohen, Trans. ASM, **49** (1957), 823.

(26) W.A. Rachinger, J. Sci. Instrum., **25** (1948), 254.

(27) S. Sato, Jap. J. Appl. Phys., **1** (1962), 210.

in this report, though the proportions of twinned martensite which was determined by an electronmicroscopy technique were about 10 percent in S38C and 15~20 percent in 25Ni specimens.

Foils for transmission electronmicroscopy were prepared by a preliminary chemical polish from one side of the surfaces and then by electropolishing. Foils were examined in an electronmicroscope at 100 kV.

Micro-Vickers hardness tests on the surface of specimen were carefully carried out in order to avoid the fatigue microcracks under the load of less than 50 g. Under these load conditions, maximum penetrated depth of pyramidal cone was, in any cases, less than 8.5 μ.

III. Experimental results and discussion

1. Half-value breadth and substructure

X-ray observation of microstructural change in martensite during low-cycle fatigue was made in the S38C and 25Ni specimens tempered at various temperatures. The results of half-value breadth change in (211)α' diffraction line are given in Figs. 2 and 3. The S38C specimens were cycled to 300 times at $\varepsilon=1.0\%$ and then were cycled further to cause failure at $\varepsilon=1.3\%$ as shown in Fig. 2.

The half-value breadth in a tempered state decreases according to the tempering temperature increases, and in the low-temperature tempered specimens, half-value breadth decreases during fatigue tests, but in the high-temperature tempered ones, it slightly increases during fatigue tests. These changing modes were observed not only in S38C specimens but also in 25Ni even at $\varepsilon=1.6\%$.

Fig. 4 shows a relation between tempering temperature and half-value breadth

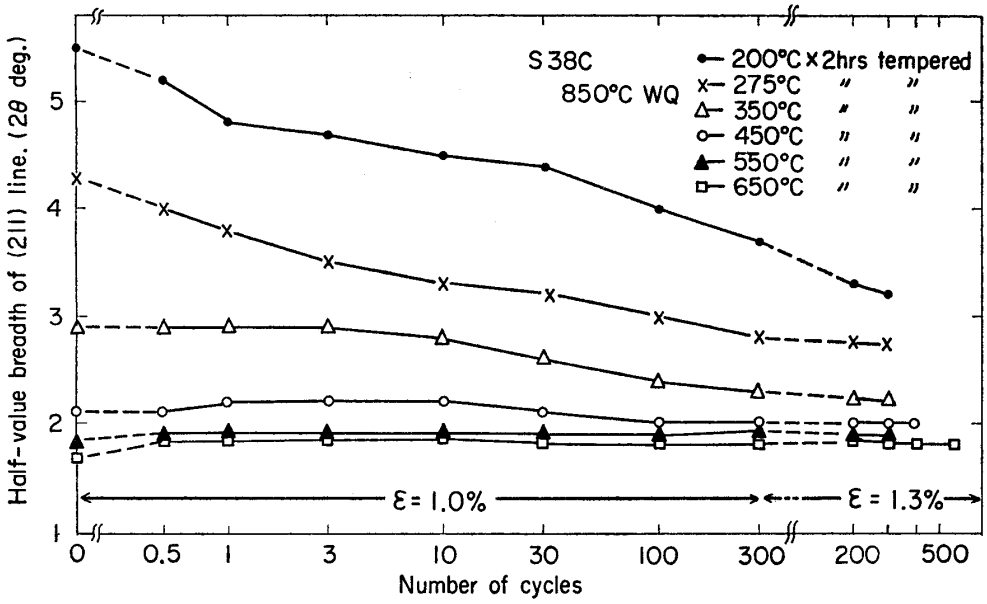

Fig. 2. Change in half-value breadth during low-cycle fatigue in S38C steel tempered at various temperatures.

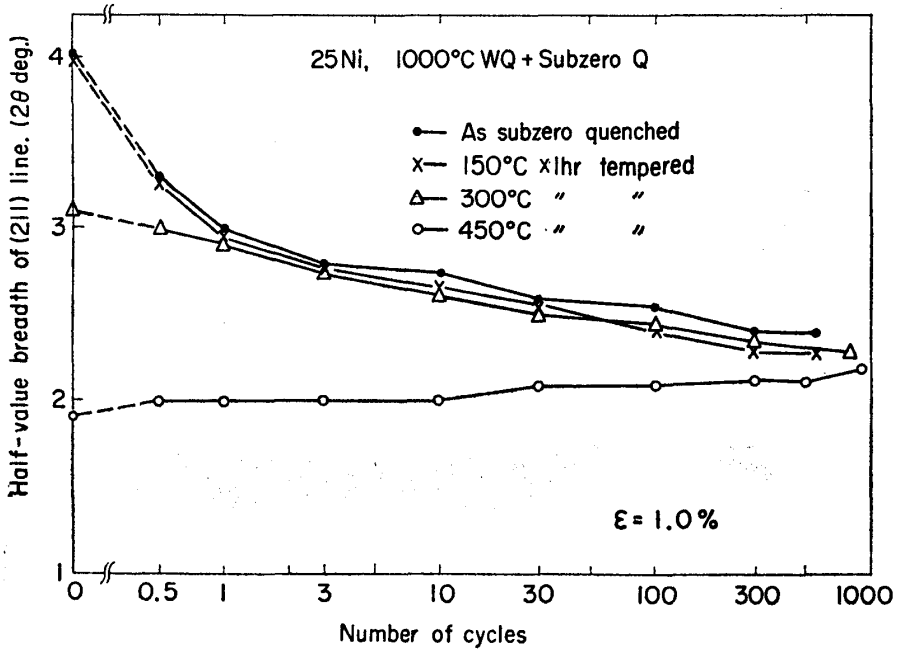

Fig. 3. Change in half-value breadth during low-cycle fatigue in 25Ni alloy tempered at various temperatures.

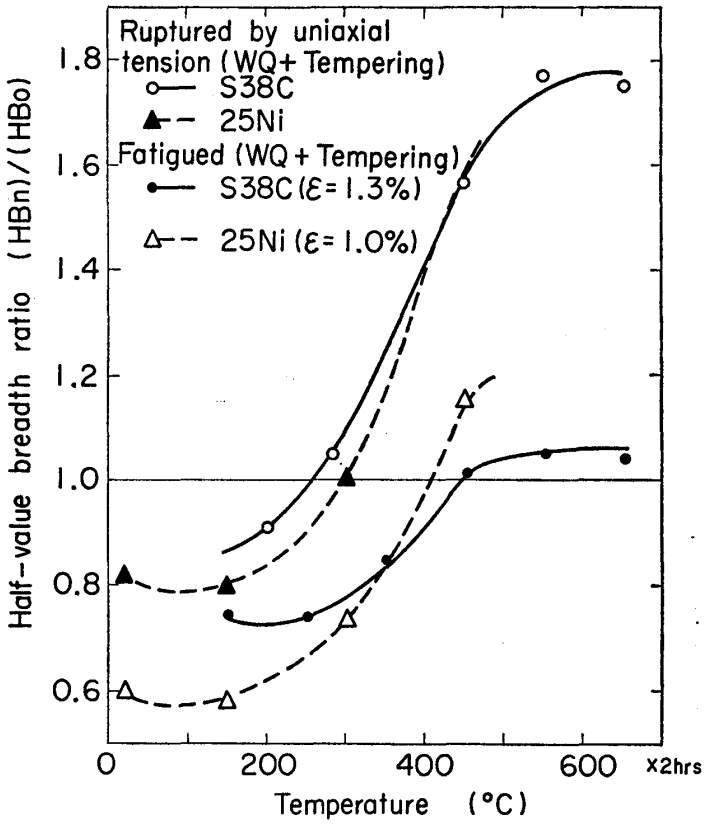

Fig. 4. Relation between tempering temperature and half-value breadth ratio in low-cycle fatigued or ruptured by uniaxial tension martensitic steels.

ratio (HB_n/HB_0) in the S38C and 25Ni specimens fatigued or ruptured by a uniaxial tension. In this case, HB_0 shows the half-value breadth in a tempered state and HB_n corresponds to that in the fatigue failured or ruptured state. It is clearly shown that there is a prominent difference in the half-value breadth change according to the failure mode, but there is a little difference in that between the S38C and 25Ni specimens. That is to say, the half-value breadth in both specimens increases, during low-cycle fatigue tests, only in the tempered states at about 400°C or above. Below this critical temperature which corresponds to about 400°C in this case, the decreasing ratio in half-value breadth during low-cycle fatigue becomes larger as the specimens are tempered at lower temperatures.

Compared with these low-cycle fatigue phenomena, in the specimens ruptured by a uniaxial tension, the critical temperature becomes about 300°C which is lower than that in the low-cycle fatigued ones.

From the result described above, it may be concluded that the critical temperature is dependent on the strain range, that is, if ε becomes larger than $1.0\sim 1.3\%$, then the critical temperature is shifted toward 300°C. Thus, in martensitic steels, the changing mode in half-value breadth is dependent on the strain range and, therefore, the half-value breadth is insufficient to presume the damage fraction in low-cycle fatigue, but the failure modes such as fatigue, rupture, etc. can be estimated by the half-value breadth. But at present another investigations are necessary to make these failure modes clear.

In addition, it is worth noting in Figs. 2 and 3 that the half-value breadth after cycling to failure converges in the 25Ni alloy in spite of the large difference in a tempered state, while in S38C steel it does not converge. It is clear that such a difference in both materials is closely related to the carbon content. In the 25Ni alloy which scarcely contains carbon atoms as few as 0.003%, the locking of dislocations by carbon atoms may be very weak compared with that in the S38C steel containing 0.38%C and, therefore, redistribution of dislocation during cycling similarly occurs in spite of the difference in tempering conditions, and their dislocation structures were expected to change into the same ones. But in the S38C steel, the states of precipitated carbides such as the kinds, size, distribution, etc. are different according to the tempering conditions, and because of these difference it may be difficult to become a same microstructure detected by X-ray diffraction method even after cycling to failure.

Photos. 1 and 2 are the results of thin film electronmicroscopy observations in the 25Ni and S38C specimens before and after low-cycle fatigue tests. It is clearly observed from these photographs that a dislocation density before fatigue tests both in S38C and in 25Ni specimens tempered below the critical temperature is higher than that tempered above the critical temperature. But in the case of 25Ni alloy, elongated subgrains are similarly formed after fatigue tests in spite of the difference in tempering temperature. This subgrain size is about $1\sim 5$ microns in width and is almost equal to the width of martensite leaves. In the case of

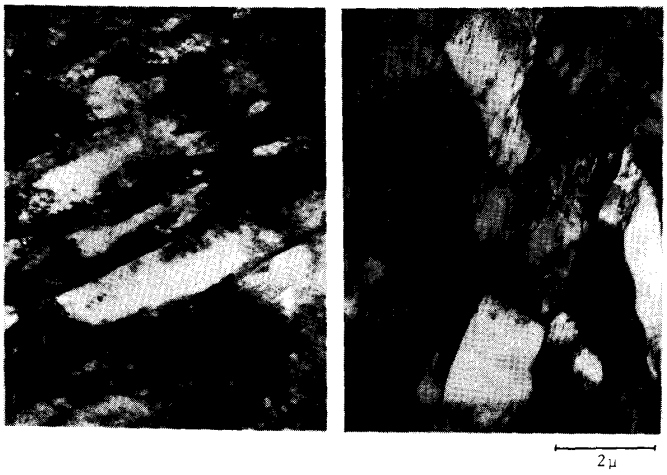

Before fatigue test After 500 cycles at $\varepsilon=1.0\%$
(a)

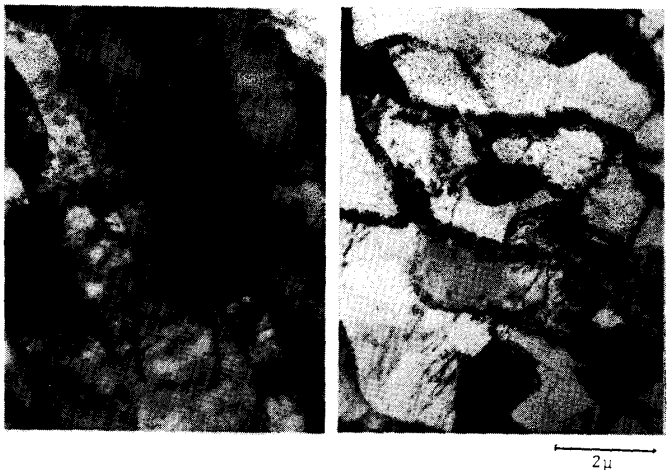

Before fatigue test After 500 cycles at $\varepsilon=1.0\%$
(b)

Photo 1. Substructure in tempered and low-cycle fatigued 25Ni alloy. (a) As quenched, (b) Tempered at 450°C.

S38C steel, elongated subgrains are formed similarly in the case of fatigued 25Ni alloy only in the high-temperature tempered sepcimens, but in the low-temperature tempered specimens, substructural changes during cycling are scarcely observed as shown in Photo. 2 (a). Though these substructural changes observed by thin film electronmicroscopy cannot be correlated directly to the changes in half-value breadth detected by an X-ray method, their changing phenomena are similar to each other.

It is clearly confirmed by the low-cycle fatigue studies on the annealed or cold-worked metals[6] that the subgrains are always formed by fatigue, regardless of the structure before cycling. Other investigators[5] concluded that the integral breadth of X-ray diffraction lines from (110) or (220) plane in low carbon annealed steel was leveled each other by the definite strain cycling.

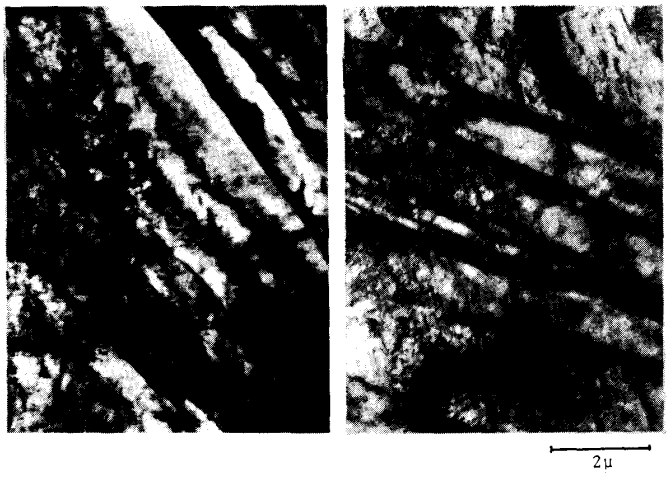

Before fatigue test After 500 cycles at $\varepsilon=1.3\%$
(a)

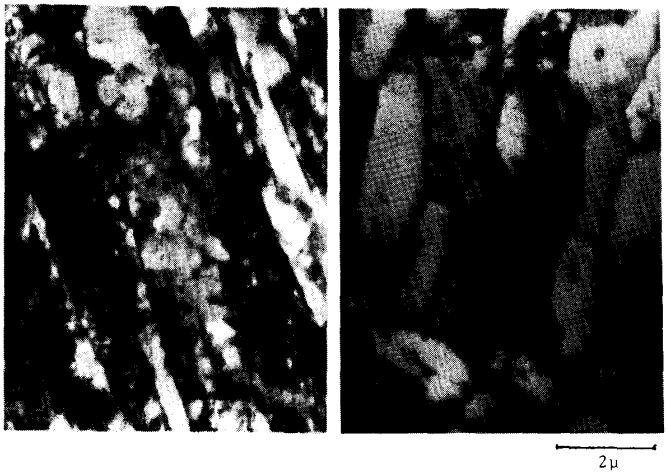

Before fatigue test After 500 cycles at $\varepsilon=1.3\%$
(b)

Photo. 2. Substructure in tempered and low-cycle fatigued S38C steel. (a) Tempered at 200°C, (b) Tempered at 550°C.

Consequently, the differences in substructure and half-value breadth during cycling are similar, only in the 25Ni alloy, to the contrast of annealed metals versus cold-worked ones, in this case, the annealed metals correspond to the specimens tempered above the critical temperature and the cold-worked metals correspond to that tempered below the critical temperature. But their differences in the S38C steel are not leveled out even after the fatigue to failure, and these phenomena are considered to characterise martensite containing carbon atoms.

2. Hardness

Relations between tempering temperature and half-value breadth or hardness in the S38C and 25Ni specimens before and after fatigue tests are given in Figs.

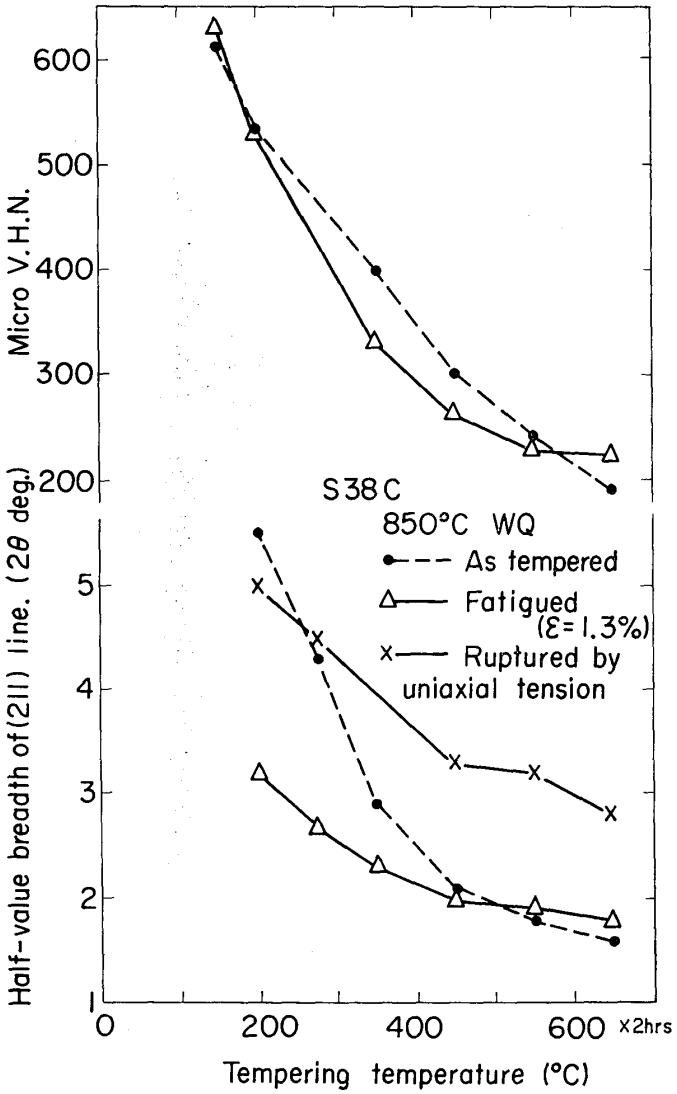

Fig. 5. Relation between tempering temperature and half-value breadth or hardness in low-cycle fatigued or ruptured by uniaxial tension S38C steel.

5 and 6 together with half-value breadth in the specimens ruptured by a uniaxial tension. In both materials, the half-value breadth is different according to the failure mode, that is, low-cycle fatigue and uniaxial tension and this phenomenon can be explained by their dependence of strain range[1] as described in Fig. 4.

Hardness in the as-tempered S38C specimens decreases with the increase of tempering temperature and its decreasing mode qualitatively corresponds to the decreasing mode of half-value breadth, but in the as-tempered 25Ni specimens, the decrease of hardness is very slight in spite of the large decrease in half-value breadth. We cannot definitely conclude this cause similarly to the mechanical properties in this alloy as described in Table 2.

Hardness in the S38C specimens fatigued to failure, only in the case of tempering above 350°C before fatigue tests, approximately decreases with the decrease

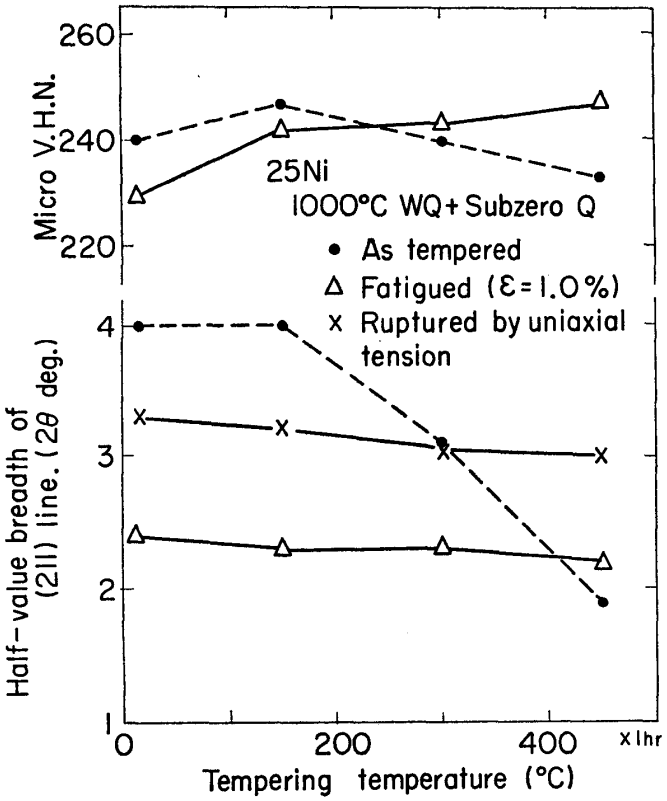

Fig. 6. Relation between tempering temperature and half-value breadth or hardness in low-cycle fatigued or ruptured by uniaxial tension 25Ni alloy.

in half-value breadth and increases to the increase of half-value breadth, but in the specimens tempered below 200°C, hardness little changes during fatigue tests with the large decrease in half-value breadth. However, it should be noted that the change of hardness during fatigue tests is not correlated in detail with the half-value breadth. The reason is that in as much as the half-value breadth was measured as a mean value on the regions including fatigue microcracks, while the hardness was measured on the regions excluding fatigue microcracks.

According to the observations on surface damage by optical microscopy, remarkable deformed regions were observed in the S38C specimens tempered above 350°C in the intermediate regions among fatigue microcracks, but these deformed regions were scacely observed in the specimens tempered below 200°C. Hence it appears that microstructure in the regions of hardness measurement little changes in the specimens tempered below 200°C and the decrease of half-value breadth in this case is due to the microstructural changes only in the extremely near region of microcracks, and it may be thought that such a phenomenon on surface damage is the cause of discrepancy, in the specimens tempered below 200°C, between hardness and half-value breadth as shown in Fig. 5. However, the specimens tempered below 200°C contains considerable carbon atoms in matrix, and the possibility of hardening due to the carbide formation or clustering of carbon atoms during fatigue tests may be expected. Therefore, more detailed experimental research is

required in order to discuss the hardness change in martensitic steel during fatigue tests.

In the case of 25Ni alloy, hardness slightly decreases by fatigue in the specimens tempered at low temperature and it decreases in the specimens tempered at high temperature similarly to the S38C specimens tempered above 350°C, but their magnitude is unexpectedly small compared with the difference in half-value breadth.

3. Particle size and microstrain

Relations between tempering temperature and the particle size (D) or microstrain ($\Delta d/d$) in the S38C and 25Ni specimens before and after fatigue tests are given in Figs. 7 and 8. On comparing these results with the changes of half-value breadth in Figs. 5 and 6, the decrease of half-value breadth by fatigue in both materials corresponds to the increase of D or the decrease of $\Delta d/d$ and the increase

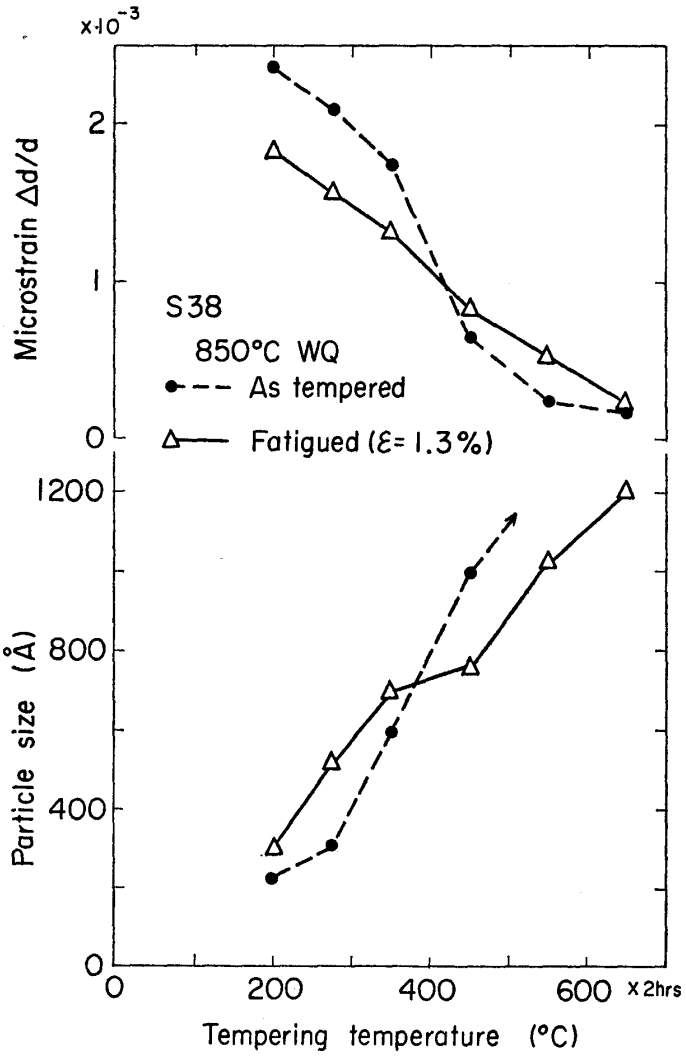

Fig. 7. Relation between tempering temperature and particle size or microstrain in tempered and fatigued S38C steel.

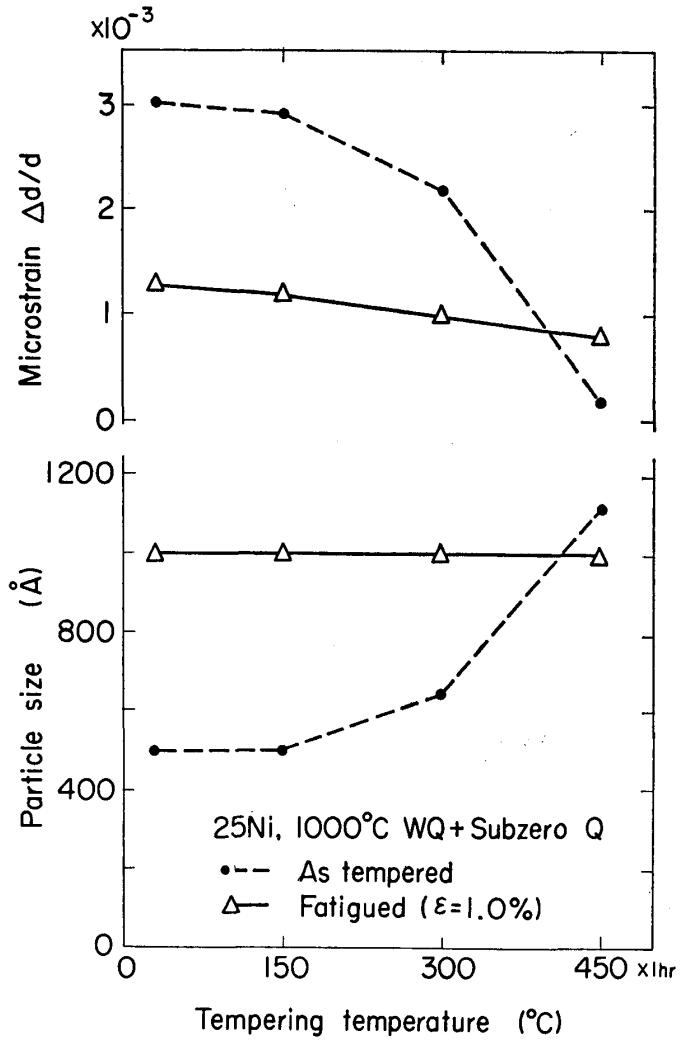

Fig. 8. Relation between tempering temperature and particle size or microstrain in tempered and fatigued 25Ni alloy.

of half-value breadth by fatigue corresponds to the decrease of D or the increase of $\Delta d/d$. In addition, it is worth noting in Figs. 7 and 8 that not only D but also $\Delta d/d$ approximately converges similarly to the half-value breadth after cycling to failure in 25Ni alloy despite of the large difference in a tempered state, and this indicates that the microstructure becomes a similar state, but in the S38C steel, they do not converge. Furthermore, D in the S38C specimens, on the whole, is smaller than that in the 25Ni specimens. This difference of D in both materials is perhaps due to the difference of carbon content.

4. Permanent deflection

Fig. 9 shows the changes in permanent deflection in the tempered S38C specimens during fatigue under $\varepsilon=1.6\%$. Only in the specimens tempered at 150°C after ice water quenching, the permanent deflection remarkably decreases

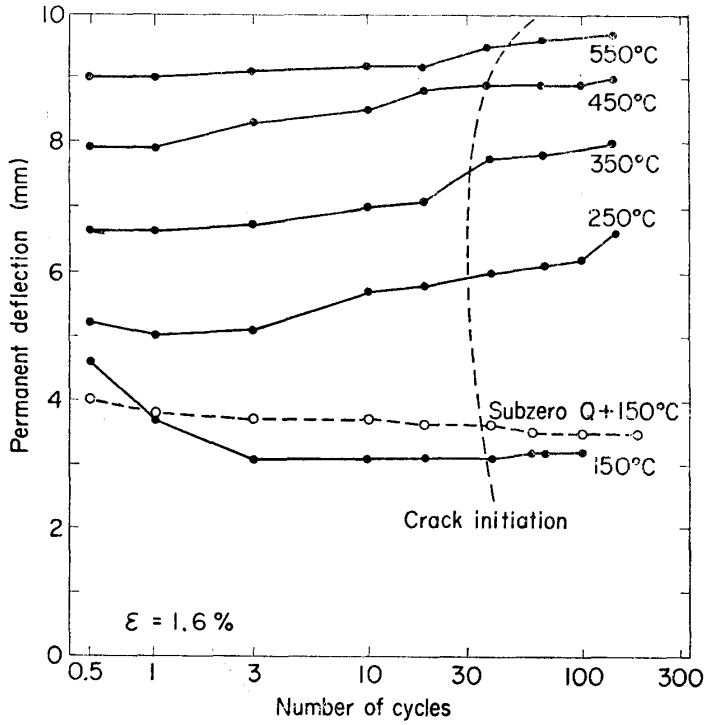

Fig. 9. Change in permanent deflection in tempered S38C steel during low-cycle fatiuge.

during the initial few cycles until the microcracks initiate, and after a few cycling it becomes constant. But in the specimens tempered at 150°C after subzero quenching at −196°C, such a decrease is not observed.

In the ice water quenched specimens, an existence of retained austenite can be detected by a dilatometric measurement, but its amount is so little that it cannot be detected by an X-ray diffraction method. Such a retained austenite may be transformed to martensite by low-cycle fatigue and then induces a transformation plasticity[28], therefore, the cause of initial decrease in permanent deflection shown in Fig. 9 may be attributed to the effect of such a plasticity.

In the specimens tempered above 250°C, the permanent deflection increases until the microcracks initiate, and their increasing degree becomes enhanced with the decrease of tempering temperature. This cause may be attributed to the softening effect in fatigue process which has been observed by the decrease of hardness, half-value breadth, etc., for example, in Fig. 5.

5. Initiation and propagation of microcracks

In recent years, Beardmore[29] reported that initiation and propagation of microcracks are independent of microstructural features, that is the prior

(28) Y. Imai and S. Kumagai, To be published in J. Soc. Mat. Sci., Japan, 20 (1971).
(29) P. Beardmore and C.E. Feltner, Fracture, (1969), 607. Proc. 2nd Inter. Conf. on Fracture, Brighton.

austenite grain boundaries, the martensite leaves and others in the low-carbon alloy martensitic steel. However, in our investigation, the initiation and propagation of low-cycle fatigue microcracks not only in the low-carbon 25Ni alloy but also in the S38C steel are evidently influenced by these microstructural features irrespective of the tempering temperature.

In general, it is said that fatigue cracks initiate from the nonmetallic inclusions in the hardened steels. Indeed, in the S38C specimens tempered at low temperature range of 150～200°C, such an initiation mode of microcracks is often observed. However, almost simultaneously with the initaition of microcracks from

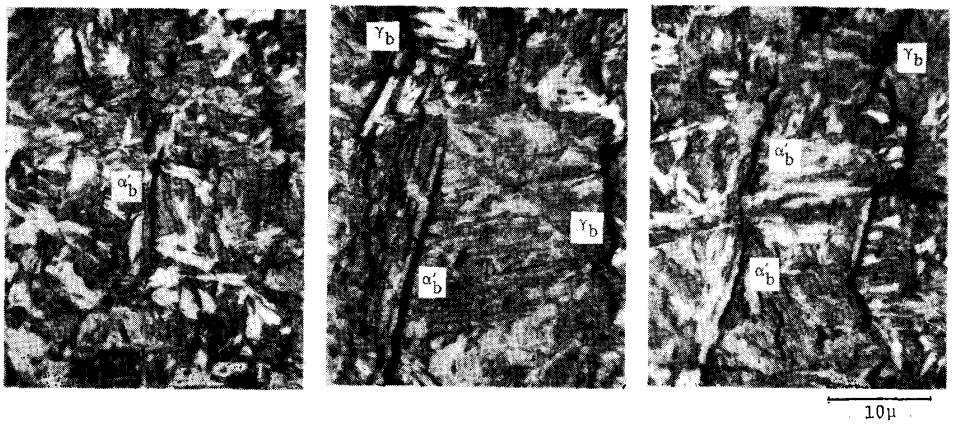

Photo. 3. Low-cycle fatigue microcracks along the edges of martensite leaves (α_b') and prior austenite grain boundaries (γ_b) in S38C steel tempered at 150°C. After 300 cycles at $\varepsilon=1.3\%$.

nonmetallic inclusions, many microcracks initiate along the edges of martensite leaves (lath boundaries), prior austenite grain boundaries and others. Examples of these results are shown in Photo. 3. These microcracks initiated in any manner preferentially propagate along the lath boundaries, prior austenite grain boundaries and others. These detailed results on the initiation and propagation of microcracks will be published[30] elsewhere.

Summary

The results obtained by X-ray diffraction and thin film electronmicroscopy methods may be summarized in two phenomena. One is similar to the contrast of annealed metals versus cold-worked metals, and the other is what is considered to characterize martensitic steels containing some amount of carbon atoms.

Both materials used in this investigation in tempered condition present a remarkable variation in microstructure and the difference in microstructure is almost leveled out only in the low carbon 25%Ni alloy by the fatigue and this phenomenon is similar to the contrast of annealed metals versus cold-worked

(30) S. Kumagai and Y. Imai, To be published in J. Soc. Mat. Sci., Japan, **20** (1971), 1114.

metals. But in the 0.38%C steel the difference is not leveled out even after the fatigue to failure. The results obtained are not yet adequate enough to explain the correlation between the microstructural variation and the damage fraction in martensitic steels.

The initiation and propagation of microcracks both in materials are often related to the lath boundaries and prior austenite grain boundaries.